JJMIE

Volume 17, Number 4, December. 2023
ISSN 1995-6665
Pages 571– 580
https://doi.org/10.59038/jjmie/170412
Editor-in-Chief: Prof. Ali M. Jawarneh

Jordan Journal of Mechanical and Industrial Engineering

A Method for Analyzing the Impact Characteristics of Elliptic Gears Based on Finite Element

Changbin Dong*, Xudong Yang, Yongping Liu

School of Mechanical and Electrical Engineering, Lanzhou University of Technology, Lanzhou 730050, P. R. China.

Received 15 Jun 2023 *Accepted 16 Aug 2023*

Abstract

The contact impact and contact stress on the tooth surface of elliptic gears are difficult to obtain, and the theory of dynamic performance analysis is not perfect, which seriously affects the widespread application of elliptic gears. To overcome the research difficulties and technical bottlenecks mentioned above, this article focuses on the dynamic meshing process of elliptic gears. Based on the theory of contact dynamics and the physical model of elliptic gear transmission, a finite element analysis method is proposed to solve the impact collision problem of elliptic gears. An accurate elliptic gear pair model was established by simulating the generation of elliptic gears by gear shaping cutters. On this basis, a finite element model for load-bearing contact and a numerical calculation model for contact stress of elliptic gears were proposed and established. The distribution patterns of contact stress, impact stress, impact resultant force, and impact time of elliptic gears were studied. The results indicate that the contact stress on the tooth surface is more sensitive to eccentricity, tooth width, and torque. The distribution of impact stress, impact resultant force, and impact time varies with the position of the gear teeth on the pitch curve. The research results can lay a theoretical foundation for the formation of the theory of elliptic gear meshing impact.

Keywords: Elliptic gear; contact impact; contact stress; impact stress; impact time.

1. Introduction

As a new type of gear transmission, non-circular gear is mainly used to transfer the non-uniform motion between the two shafts, and realize the nonlinear relationship between the rotation angles of the driver and the follower [1]. Noncircular gear is different from cylindrical gear because its pitch curve is non-circular. On the basis of following the advantages of cylindrical gear transmission, it has the characteristics of strong bearing capacity, compact structure, good dynamic balance, high precision, and can realize speed ratio transmission. It is mainly used in agriculture, textile, instrumentation, navigation ships and other low-speed and high torque occasions [2, 3], and elliptic gear is the most common.

In the process of gear meshing, due to machining error, installation error, and load-bearing deformation of tooth profile, the gear will mesh outside the theoretical meshing line at the initial meshing position, resulting in meshing impact.[4] The existence of tooth side clearance makes the gear also produce impact in the meshing process. In fact, the two involute tooth profiles meshing with each other will also cause certain impact due to the difference of the relative contact speed in the transient normal direction. The above impact can be summarized as the impact produced during gear meshing, that is, meshing contact impact. The meshing impact produced by gear meshing process has a great impact on the stability of gear transmission system, while the special application of non-circular gear and the inconsistency of tooth profile make the meshing process more complex. Therefore, it is necessary to carry out systematic analysis. Many scholars study the dynamic meshing contact characteristics of gears by analytical method and finite element method, and the finite element method is the most widely used one. Munro [5] analyzed the meshing characteristics of gears with edge contact and the influence of meshing impact on transmission error of gear system, which provides a new approach for studying the dynamic characteristics of gears with edge contact. Ziegler [6] analyzed the meshing impact caused by speed at different meshing positions, and obtained the relationship between impact time and meshing stiffness with meshing position, but only numerical simulation was conducted without relevant validation. Lin [7] proposed a mesh generation method for gear transmission at any meshing position, and introduced tooth side clearance into the meshing impact model. The influence of different backlash on gear meshing impact characteristics was analyzed, which laid the foundation for analyzing the meshing impact characteristics of gear transmission systems under time-varying backlash excitation. Zhou [8] established a gear line external meshing impact friction model, and proposed a method for obtaining the impact friction force and friction coefficient at the contact point, which provides a new method for improving the meshing impact theory of gear transmission systems under friction conditions. Tang [4] proposed using ANSYS/LS-DYNA to simulate the dynamic meshing process of gear teeth for studying the meshing impact problem of

* Corresponding author e-mail: lutdcb@126.com.

gears, but did not consider the coupling excitation effect between gear teeth under load-bearing contact conditions. On this basis, Tang [9] proposed the concept of gear transmission meshing contact impact and studied the phenomenon of gear tooth contact impact caused by speed differences at meshing points, but the influence of gear tooth distribution position on it was not considered in the analysis. Al-Shyyab [10] and Ahmad [11] proposed to combine the meshing impact of gears with the torsional dynamic model of multi-stage planetary transmission systems, and analyzed the dynamic characteristics of gear transmission systems under impact excitation, which built a bridge for the meshing impact and nonlinear characteristics of gear transmission systems. Zhang [12] proposed using gear profile modification and tooth orientation modification to address the NVH problem of automotive transmissions, and compared and verified them using finite element analysis, which indicates that gear modification can be an important measure to reduce impact fluctuations. Gao [13] established an elliptic gear meshing mathematical model to analyze its nonlinear vibration characteristics and instability, and provided some guidance for subsequent non-circular gear meshing shock analysis. Literature[14] analyzed the meshing characteristics of gear under actual working conditions by establishing dynamic meshing models of elliptic gears, but not mentioned the impact of meshing in and out. Many literatures [15-19] use finite element analysis methods to solve collision and contact problems, as well as the calculation of related stress-strain coefficients, which indicating that finite element analysis methods can be used as an analytical tool for complex surface contact problems.

The above-mentioned research results are of great significance to the analysis of the meshing contact impact of elliptic gears. At present, there is almost no comprehensive literature on the meshing impact characteristics of elliptic gears. Therefore, the article will propose and establish a finite element model for the meshing contact impact analysis of the elliptic gear pairs, and explore the distribution law of the resultant impact force, impact stress and impact time. The change trend of the contact stress with the position of the tooth on the pitch curve. It is expected to provide a certain theoretical basis for the engineering application and vibration and noise reduction of elliptic gears.

2. Mathematical models of contact stress and meshing impact

2.1. Tooth surface contact stress of elliptic gear

Based on the Hertz contact theory, the meshing of the two gears can be simplified as the contact problem of two cylinders with equivalent time-varying radii. As shown in Figure 1, N_1N_2 is the theoretical meshing line and r_1, r_2 are the driving and driven gear pitch curve radius and r_{b1}, r_{b2} are the base circle radius of the driving and driven gears. The contact stress of the gear pair at the meshing point P is:

$$\sigma_p = \sqrt{\frac{F_p}{\pi\rho_p\left(\frac{1-\nu_1^2}{E_1}+\frac{1-\nu_2^2}{E_2}\right)}} \tag{1}$$

$$\rho_p = \frac{\rho_1\rho_2}{\rho_1+\rho_2} \tag{2}$$

In the above formula, F_p is the load on the unit contact line length of the teeth. ρ_p is the overall radius of curvature. ρ_1, ρ_2 are the radius of curvature of the driving and driven gears at the meshing point respectively. E_1, E_2 are the elastic modulus of the driving and driven gear respectively. ν_1, ν_2 are the driving and driven gear Poisson's ratio, respectively.

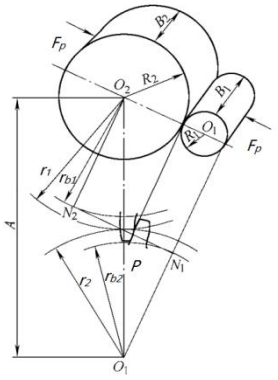

Figure 1. Contact model of gear pair

In a gear meshing cycle, there are two double teeth meshing areas and a single tooth meshing area, and the single tooth meshing area is located between the two double teeth meshing areas. In the single tooth meshing area, the load is borne by a single tooth, While in the double teeth meshing area, the load is borne by two teeth. Therefore, the load distribution coefficient Z_L is to be introduced to characterize the distribution of contact stress during gear meshing. The calculation method of the starting position pressure angle and the ending position pressure angle of the single tooth meshing area has been described in detail in reference [20], and will not be repeated here. Therefore, the contact stress of the tooth surface of the elliptic gear can be expressed as：

$$\sigma = \begin{cases} \sigma_p & \text{(Single tooth)} \\ Z_L\sigma_p & \text{(Double tooth)} \end{cases} \tag{3}$$

2.2. Meshing contact impact theory

Figure 2 shows that two elastic bodies and are in contact at point C. From the start of meshing time t_0 to the end time t_1, the motion control equation of the system is:

$$M(\dot{U}_1-\dot{U}_0)+\lim_{t_1\to t_0}\int_{t_0}^{t_1}(C\dot{U}+KU-F-R)dt=0 \tag{4}$$

Where M, C, K, F and are the mass matrix, damping matrix, stiffness matrix, load vector and contact force of elastic bodies Ω_1 and Ω_2 respectively. U and $\dot{U}$ are the displacement and velocity of Ω_1 and Ω_2 respectively.

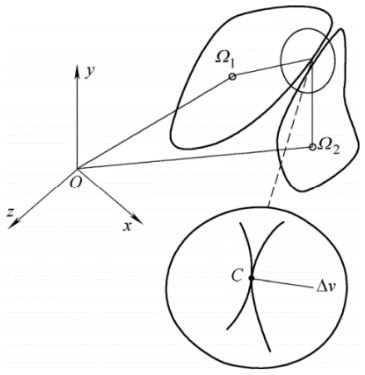

Figure 2. Elastic body contact

It can be seen from formula (4) that when the speed difference between the two elastic contact bodies is small, the speed of the system remains basically unchanged or changes very little. At this time, the contact process of the two elastic bodies will continue for a period of time. The effect is similar

to other forces, which is the continuous contact between two elastomers. On the contrary, when two elastic bodies contact each other with a certain speed difference, the system speed will change suddenly and the contact time is very short, which will produce a large contact force, which is the contact impact when the two elastic bodies are in contact.

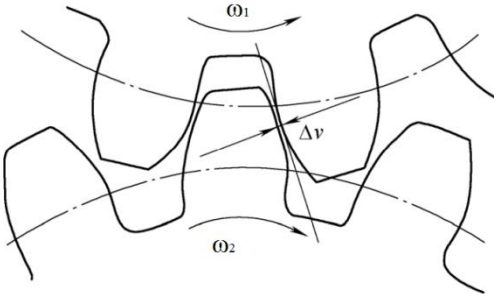

Figure 3. Gear transmission physical model

Figure 3 shows the physical model of the elliptic gear meshing transmission. At this time, the gear contact impact can be regarded as the impact generated when two elastic contact bodies are in contact. When the elliptic gear works normally, the tooth profile of the driving gear pushes the tooth profile of the driven gear to achieve meshing motion. Therefore, it will move according to the predetermined transmission ratio under ideal conditions, so as to ensure that there is only tangential relative speed between the two gears at the contact point, and the normal relative speed $\Delta v = 0$. Therefore, the contact between the teeth during gear transmission presents continuous contact between two elastomers.

2.3. Finite element analysis method for meshing contact impact of elliptic gear

The basic motion equation of the gear system dynamics analysis is :

$$M\ddot{U} + C\dot{U} + KU = F \tag{5}$$

LS-DYNA uses the central difference method to solve the motion differential equation of dynamic problems. The essence of the central difference method is to replace the differential with the difference, namely:

$$\begin{cases} \ddot{U}_t = \dfrac{1}{\Delta t^2}(U_{t-\Delta t} - 2U_t + U_{t+\Delta t}) \\ \dot{U}_t = \dfrac{1}{2\Delta T}(-U_{t-\Delta t} + U_{t+\Delta t}) \end{cases} \tag{6}$$

Taking equation (6) into dynamic differential equation (5), the system of linear equations can be obtained

$$\bar{M}U_{t+\Delta t} = \bar{R}_t \tag{7}$$

$$\bar{M} = \frac{1}{\Delta t_2}M + \frac{1}{2\Delta t}C$$

$$\bar{R}_t = F_t - (K - \frac{2}{\Delta t^2}M)U_t - (\frac{1}{\Delta t^2}M - \frac{1}{2\Delta t}C)U_{t-\Delta t}$$

Where $\bar{M}$ is the effective mass matrix and $\bar{R}_t$ is the effective load vector.

According to equation (7), the state parameters of $t+\Delta t$ time can be calculated from the state quantities of $t-\Delta t$ and t time, which is the characteristic of display algorithm.

The time step size of the algorithm is limited by the element size, so it is necessary to establish a reasonable and accurate finite element model to improve the calculation accuracy. In contrast, using LS-DYNA software to simulate the dynamic meshing process of gear teeth by establishing a nonlinear contact element in the meshing area is more in line with the actual working conditions. The parameters of elliptic gear are shown in Table 1.

2.4. Mathematical model of elliptic gear

Figure 4 shows the basic principle of using gear shaper cutter as gear cutter to produce elliptic gear. The principle of tooth profile envelope is ensuring the pure rolling of a pair of elliptic gear pitch surfaces, the other cylindrical gear contacts the pure rolling elliptic gear pitch surfaces instantaneously and ensures the pure rolling relationship.

Table 1. Elliptic gear design parameters

Parameter	Value
Module m (mm)	3
Number of teeth z	47
Center distance a (mm)	145
Addendum coefficient *ha**	1
Top clearance coefficient *C**	0.25
Tooth width B (mm)	30
Eccentricity *e*	0.3287
Pressure angle (°)	20
Equation of pitch curves	$r = \dfrac{64.667}{1 - 0.3287\cos\varphi}$

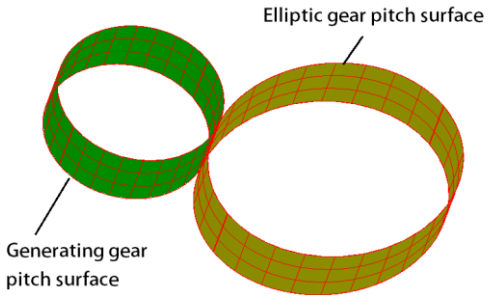

Figure 4. Basic principle of generating elliptic gear with cylindrical gear shaper cutter

The tooth profile of elliptic gear is involute. For involute profile gear transmission, the section of gear shaper cutter is involute, and the section equation is:

$$\begin{cases} x_g(u) = r_{gb}(\cos u + u\sin u) \\ y_g(u) = r_{gb}(\sin u - u\cos u) \end{cases} \tag{8}$$

Where r_{gb} is the radius of the base circle; μ is the included angle between the tooth profile of the gear shaper cutter and the X axis in the coordinate system of the gear shaper cutter.

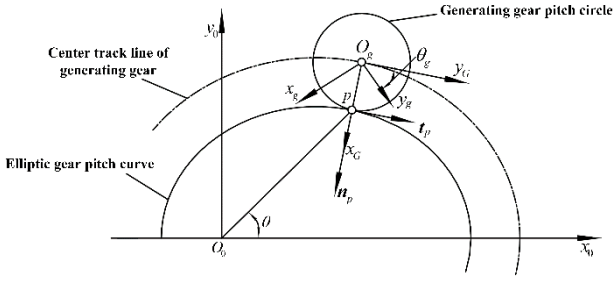

Figure 5. The coordinate transformation relationship of generating elliptic gear

According to the gear meshing principle, the generating gear and the generated gear meet the pure rolling relationship, that is, the gear shaper pitch curve and the elliptic gear pitch

curve are in instantaneous tangent contact. Therefore, the coordinate system can be established through the tangent vector and normal vector of the elliptic gear pitch curve to construct the motion relationship between the coordinate systems. Based on the basic idea of the motion inversion method, assuming that the elliptic gear is fixed, the relationship among the gear shaper cutter coordinate system, and the elliptic gear coordinate system and the auxiliary coordinate system at the contact point P of the gear shaper cutter can be defined. Figure 5 shows the coordinate conversion relationship when forming the elliptic gear. Figure 5 contains the following three coordinate systems:

1. $S_0(O_0 - x_0y_0z_0)$ is the fixed coordinate system, which is fixed on the elliptic gear to be produced. The rotation angle of the elliptic gear is expressed as θ, and the pitch curve equation is defined as $r_p(\theta)$.

2. $S_G(O_g - x_Gy_Gz_G)$ is the auxiliary coordinate system, which is determined by the normal and tangential directions of the elliptic gear pitch curve and the contact point P of the production tool (gear shaper) and the center of the production wheel. The center of the generating gear is the point of the radius of the normal gear shaper cutter. Using the vector coordinate transformation, the unit vectors of the three coordinate axes of the coordinate system S_p can be expressed as:

$$\begin{cases} \boldsymbol{i}_{\mathrm{p}}(\theta) = \boldsymbol{n}_{\mathrm{p}}(\theta) \\ \boldsymbol{j}_{\mathrm{p}}(\theta) = \boldsymbol{t}_{\mathrm{p}}(\theta) \\ \boldsymbol{k}_p(\theta) = [0\ 0\ 1]^{\mathrm{T}} \end{cases} \tag{9}$$

The unit vectors of the three coordinate axes of the coordinate system S_0 can be expressed as:

$$\begin{cases} \boldsymbol{i}_0 = [1\ 0\ 0]^{\mathrm{T}} \\ \boldsymbol{j}_0 = [0\ 1\ 0]^{\mathrm{T}} \\ \boldsymbol{k}_0 = [0\ 0\ 1]^{\mathrm{T}} \end{cases} \tag{10}$$

There are the following coordinate transformations between coordinate system S_G and coordinate system S_0:

$$\boldsymbol{M}_{0\mathrm{G}}(\theta) = \begin{bmatrix} \boldsymbol{n}_{\mathrm{p0}} & \boldsymbol{t}_{\mathrm{p0}} & 0 & \boldsymbol{r}_{\mathrm{og0}} \\ \boldsymbol{n}_{\mathrm{p1}} & \boldsymbol{t}_{\mathrm{p1}} & 0 & \boldsymbol{r}_{\mathrm{og1}} \\ 0 & 0 & 1 & 0 \\ 0 & 0 & 0 & 1 \end{bmatrix} \tag{11}$$

3. $S_g(O_g - x_gy_gz_g)$ is the gear shaper cutter coordinate system, which is fixed on the gear shaper cutter. In Figure 5, the rotation angle relative to the coordinate system S_p is the rotation angle of the gear shaper cutter, and its value can be calculated according to the pure rolling relationship of the pitch curve by the following formula:

$$\theta_g = \frac{S_{pg}(\theta)}{r_{gp}} = \frac{\int_0^{\theta} \left| \frac{\mathrm{d}r_p(\theta)}{\mathrm{d}(\theta)} \right| \mathrm{d}(\theta)}{r_{gp}} \tag{12}$$

Where $S_{pg}(\theta)$ represents the arc length of the elliptic gear pitch curve from the starting position to the current position. Thus, the coordinate transformation from the gear shaper cutter coordinate system S_G to the relative coordinate system S_P can be obtained as follows:

$$\boldsymbol{M}_{\mathrm{Gg}}(\theta_g) = \begin{bmatrix} \cos\theta_g & \sin\theta_g & 0 & 0 \\ -\sin\theta_g & \cos\theta_g & 0 & 0 \\ 0 & 0 & 1 & 0 \\ 0 & 0 & 0 & 1 \end{bmatrix} \tag{13}$$

According to equations (11) and (13), the coordinate transformation from the gear shaper coordinate system to the elliptic gear coordinate system can be obtained as follows:

$$\boldsymbol{M}_{0\mathrm{g}}(\theta) = \boldsymbol{M}_{0\mathrm{G}}(\theta)\boldsymbol{M}_{\mathrm{Gg}}(\theta_g) \tag{14}$$

Based on the above profile motion analysis of the gear cutter, the tooth profile of the elliptic gear can be obtained. By transforming the tooth surface of the profile wheel to the gear coordinate system, the envelope equation of the elliptic gear can be obtained as follows:

$$\boldsymbol{R}_{\mathrm{Eg}}(\theta,u,v) = \boldsymbol{M}_{0\mathrm{g}}(\theta)\boldsymbol{R}_{\mathrm{g}}(u,v) \tag{15}$$

The boundary of equation (15) is the tooth profile surface of elliptic gear. Generally, its meshing equation is:

$$\boldsymbol{M}_{\mathbf{0g}}(\theta)\boldsymbol{n}_{\mathbf{rg}}(u,v)\cdot v_g = \mathbf{0} \tag{16}$$

Since the gear coordinate system S_0 is fixed, the relative speed of the meshing point is the speed of the point in the forming wheel coordinate system. The motion of the auxiliary coordinate system S_G along the pitch curve of the elliptic gear and the motion of the generating gear can synthesize the relative speed at the meshing point, so the relative speed is:

$$v_{\mathrm{g}}(\theta,u,v) = t_p(\theta) + \left[0 \quad 0 \quad \mathrm{d}\theta_g / \mathrm{d}\theta\right]^{\mathrm{T}} \times \boldsymbol{R}_g(u,v) \tag{17}$$

By substituting equation (17) into equation (16), the instantaneous meshing line between the elliptic gear and the generating gear at any time can be solved, so as to form the tooth profile of the elliptic gear.

3. Contact stress analysis of elliptic gear

During the gear meshing process, the contact points are not all points on the tooth profile, but a range interval, in which pressure angle will change with the position of each point on the tooth profile. The pressure angle is an important index that affects the gear pair transmission, and the pressure angle corresponds to the meshing point on the tooth profile. Therefore, characterizing the position of the point on the tooth profile by the pressure angle is more conducive to showing the change of contact stress at each meshing point of the tooth profile.

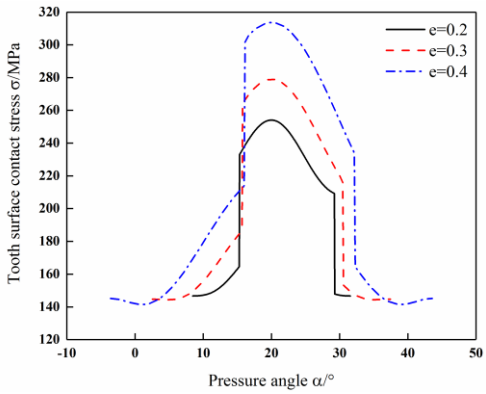

Figure 6. Influence of eccentricity on contact stress of tooth surface

With the change of eccentricity, the change trend of contact stress is shown in Figure 6. The contact stress will change suddenly in the alternating area of single and double teeth. The contact stress in the double tooth meshing area is smaller, and in the single tooth meshing area is larger. The maximum contact stress occurs at the node of single tooth contact area. With the increase of the eccentricity, the contact stress in the

single and double tooth meshing area increases. In the single tooth meshing area, the increase of contact stress is more significant, and the maximum contact stress is still located at the node of the tooth meshing area. The reason is that with the increase of eccentricity, the curvature radius of elliptic gear profile also changes. The meshing and collision of different tooth shapes will intensify the wear of the tooth surface, thereby increasing the contact stress on the tooth surface.

Due to the time-varying curvature radius of pitch curve and tooth profile of elliptic gear, each tooth profile is different, which is difficult to analyze the contact stress of tooth surface. The working area of tooth profile of non-circular gear represented by elliptic gear is generally near pitch curve, and it can be seen from Figure 6 that the maximum contact stress of tooth surface is at the pressure angle equal to 20 °, that is, the pitch curve. Therefore, in order to obtain the change trend of tooth surface contact stress with the position of gear tooth on pitch curve, the point at the intersection of pitch curve and tooth profile of elliptic gear is selected as the research object. The influence trend of eccentricity, torque and tooth width on the contact stress is obtained, as shown in Figure 7 to Figure 9.

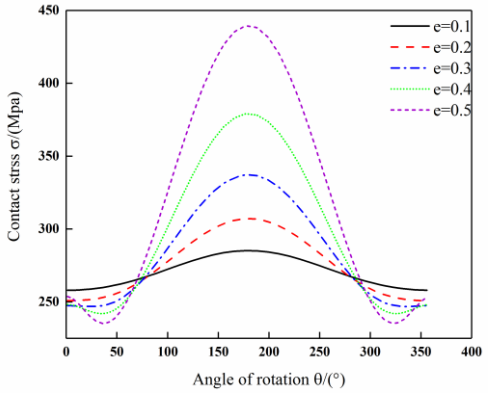

Figure 7. Influence of eccentricity on maximum contact stress of tooth surface

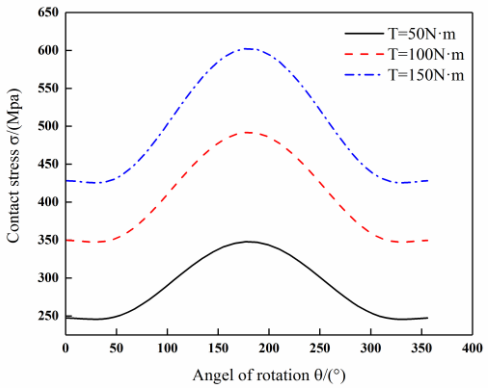

Figure 8. Influence of input torque on maximum contact stress of tooth surface

Figure 7 shows the distribution trend of the maximum contact stress on the tooth surface under different eccentricity. The contact stress curve is an approximate sine and cosine curve with continuous change. When the driving gear rotates for one cycle, the contact stress changes periodically with the rotation angle. With the increase of eccentricity *e*, the change of contact stress is more severe, and the maximum value increases and the minimum value decreases, which make the contact stress differ greatly in different driving gear angle positions and may cause premature failure of some teeth. Therefore, excessive *e* value should be avoided in practical engineering application. With the change of *e*, the θ position corresponding to the maximum contact stress almost does not change, while the θ position corresponding to the minimum contact stress will move slightly with the increase of *e*.

Figure 8 shows the variation trend of tooth surface contact stress under different input torque conditions. With the increasing of input torque, the contact stress of tooth surface shows an increasing trend, and the reason is that the increase of input torque increases the load on the unit contact line and the contact pressure on the tooth surface. In Figure 9, the maximum contact stress tends to decrease with the increase of tooth width. Due to the increase in tooth width, the length and contact area of the gear contact line gradually increase, leading to a decrease in tooth contact stress. Therefore, increasing the tooth width can reduce the contact stress on the tooth surface under the given motion law and design conditions.

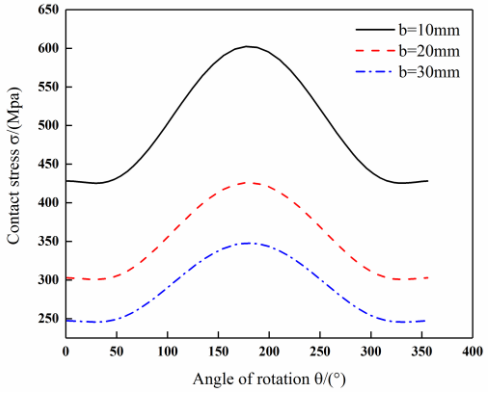

Figure 9. Influence of tooth width on maximum contact stress of tooth surface

4. Meshing contact impact analysis of elliptic gear

4.1. Finite element model of elliptic gear

In order to analyze the meshing contact impact of elliptic gear, it is necessary to establish an accurate gear model. In this paper, according to the gear meshing principle, the standard profile gear model is established in MATALB. According to the involute profile equation of the target gear, the enveloping process of the gear is simulated to obtain the coordinate data points of the elliptic gear, and then the accurate three-dimensional model is established. Figure 10 shows the elliptic gear model enveloped by the gear shaper cutter.

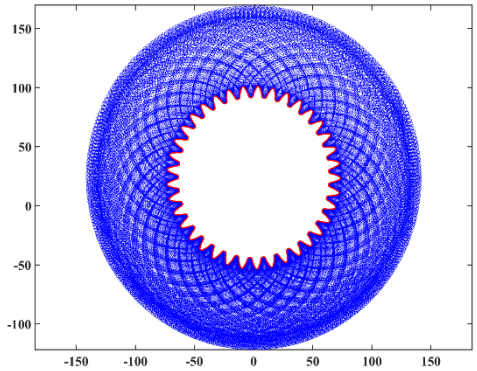

Figure 10. Envelope diagram of elliptic gear

In order to simulate the actual tooth contact in the process of meshing, the following boundary conditions should be set: the gear material is Solid164 flexible body, the inner ring material of shaft hole is Shell163 rigid body. The driver and driven wheels limit the degrees of freedom of movement in three directions of X, Y and Z and the degrees of freedom of rotation in X and Y. The rotational speed of the driver wheel is

10 r/s. The time step ratio factor TSSFAC is 0.5, and the time step DT2MS is -2e-009. Figure 11 shows the established contact finite element model of elliptic gear. Argyris [20] points out that the tooth surface presents elliptic contact area in the process of tooth meshing, and puts forward the calculation method of the corresponding elliptic contact area. When using LS-DYNA software to simulate the engagement of elliptic gear teeth, the contact area presented by the tooth surface is shown in Figure 12, which is similar to the elliptic contact area proposed in reference [22].

Since the tooth profile of the elliptic gear is different, it is time-consuming and difficult to analyze each tooth. Therefore, according to the different distribution position of gear teeth on pitch curve, the distribution law of meshing impact along pitch curve can be studied. The position of data acquisition for tooth number and tooth width direction is shown in Figure 13.

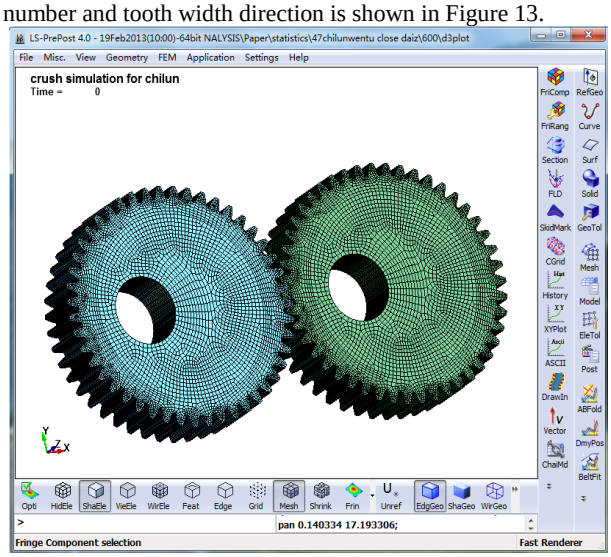

Figure 11. Finite element model of meshing contact of elliptic gear

4.2. Contact impact stress analysis of elliptic gear pair

In the meshing process of elliptic gear, the distribution law of impact stress along the tooth width direction is shown in Figure 14. The impact stress at the three data acquisition points is basically showing the same change trend. Because the elliptic gear pair used in this paper takes a focus of the ellipse as the center of rotation, and the angle between each tooth profile and the center of rotation is different, it leads to the difference of impact stress of each tooth profile. While the change trend of three data acquisition points on each tooth is consistent.

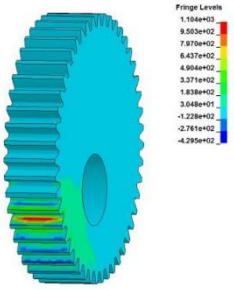

Figure 12. Elliptic contact area of tooth surface

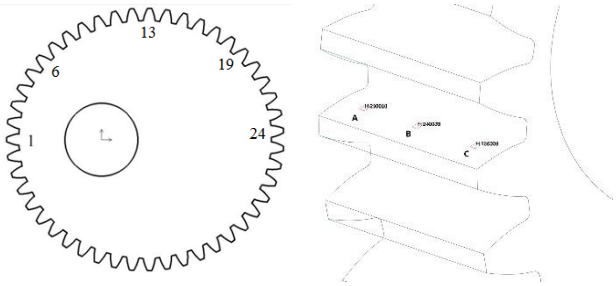

Figure 13. Tooth number and position of data acquisition point in tooth width direction

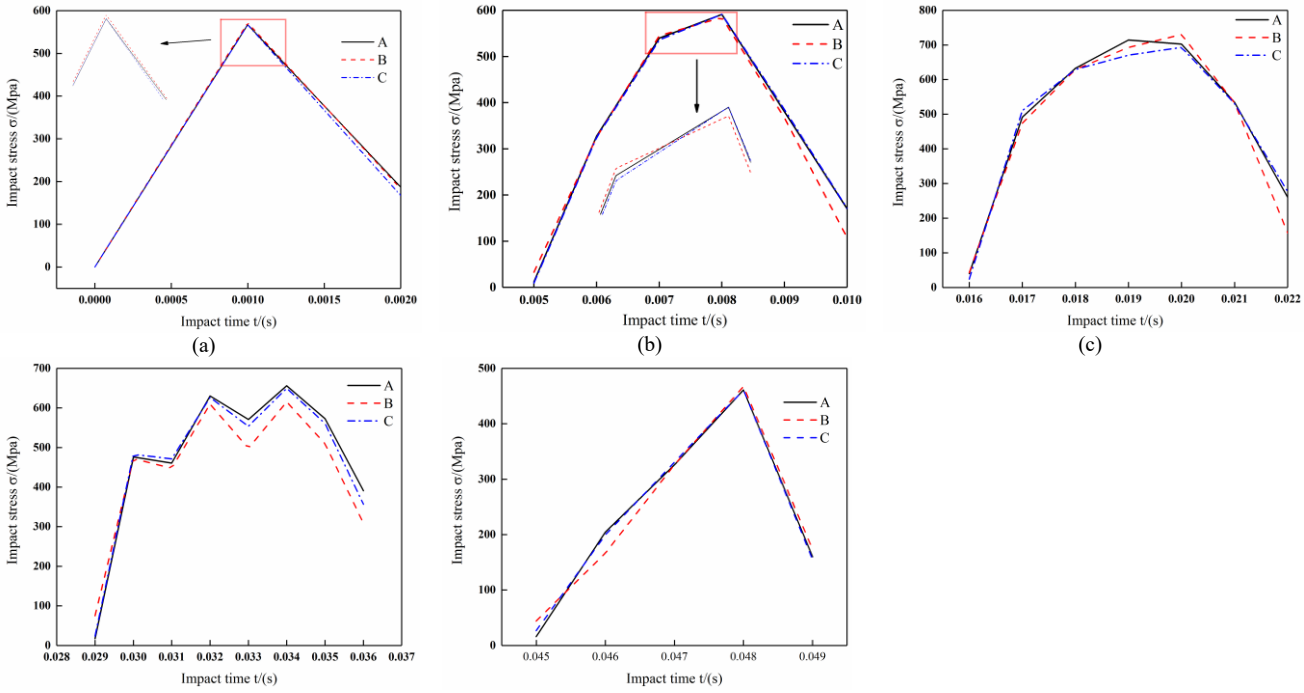

(a) ~ (e) represents No. 1, No. 6, No. 13, No. 19 and No. 24 tooth respectively

Figure 14. Impact stress along tooth width direction

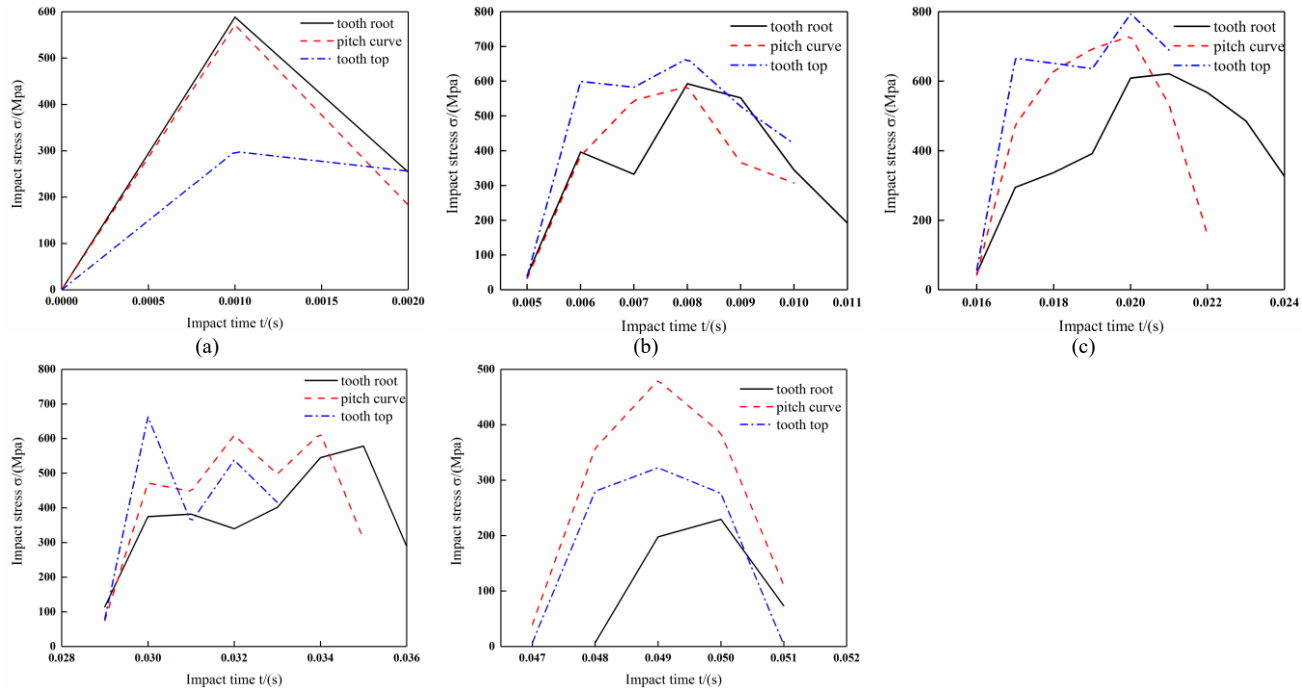

(a) ~ (e) represents No. 1, No. 6, No. 13, No. 19 and No. 24 tooth respectively

Figure 15. Impact stress along tooth height direction

The position of No.1 tooth and No.24 tooth are respectively located at the minimum curvature radius of pitch curve. It is close to the tooth profile of equivalent cylindrical gear and similar to that of ordinary cylindrical gear, so the change trend of these two teeth is relatively stable. However, the position difference of the other three teeth on pitch curve is large, which makes the curvature radius of the left and right tooth profile change more significantly, so there will be inconsistency. Especially in the impact stress curve of No.19 tooth, there are many peaks. The reason is that there are alternate areas of single tooth meshing and double tooth meshing. Further summarizing the distribution pattern in the figure, we can obtain that the impact stress increases gradually from the two ends of the long axis to the two ends of the minor axis of the elliptic pitch curve.

The distribution pattern of impact stress along the tooth height direction of elliptic gears is depicted in Figure 15. Some curves have many turns, and the reason is that the number of teeth meshed at this time is constantly changing, which is closely related to the instantaneous coincidence degree of elliptic gears. Along the direction of tooth profile, the impact stress increases gradually from root to top. As far as the distribution position of gear teeth on pitch curve is concerned, the impact stress tends to increase gradually from both ends of long axis of elliptic pitch curve to both ends of short axis. The largest change of impact stress is at the root of the tooth, followed by the top of the tooth. In contrast, the increase of meshing contact impact stress near pitch curve is the smallest, and the changes are relatively gentle.

4.3. Analysis of the resultant impact force of elliptic gear

In an elliptic gear transmission system, due to the inconsistent tooth profile, the area of elastic deformation of the tooth surface is larger than that of ordinary cylindrical gears. The area of each contact area is also changing at all times, and the contact pressure is distributed in this tiny contact area. The focus of most scholars is often the study of contact stress. In fact, the resultant impact force in the process of gear meshing is also worthy of in-depth study. For example, the study of the distribution law of the resultant impact force along the pitch curve of the gear teeth can be used for elliptic gear modification, dynamic load distribution and the determination of the load partition coefficient. Therefore, in the following, relevant research will be carried out on the resultant impact force of the elliptic gear pair when the meshing impact occurs.

During the meshing process of the elliptic gear pair, the change trend of the resultant impact force generated by the meshing impact along the tooth line is shown in Figure 16. The analysis shows that due to the inconsistency of the tooth profile, the resultant impact force of each tooth also shows a different distribution law along the tooth width direction. The resultant impact force reaches the maximum at the center of the elliptic contact area (point B), and gradually decreases from the center area to both sides. With the different positions of the teeth on the elliptic pitch curve, the distribution trend of the resultant impact force also has a certain difference, and showing a trend of gradually increasing from both ends of the long axis of the elliptic nodal curve to the ends of the short axis.

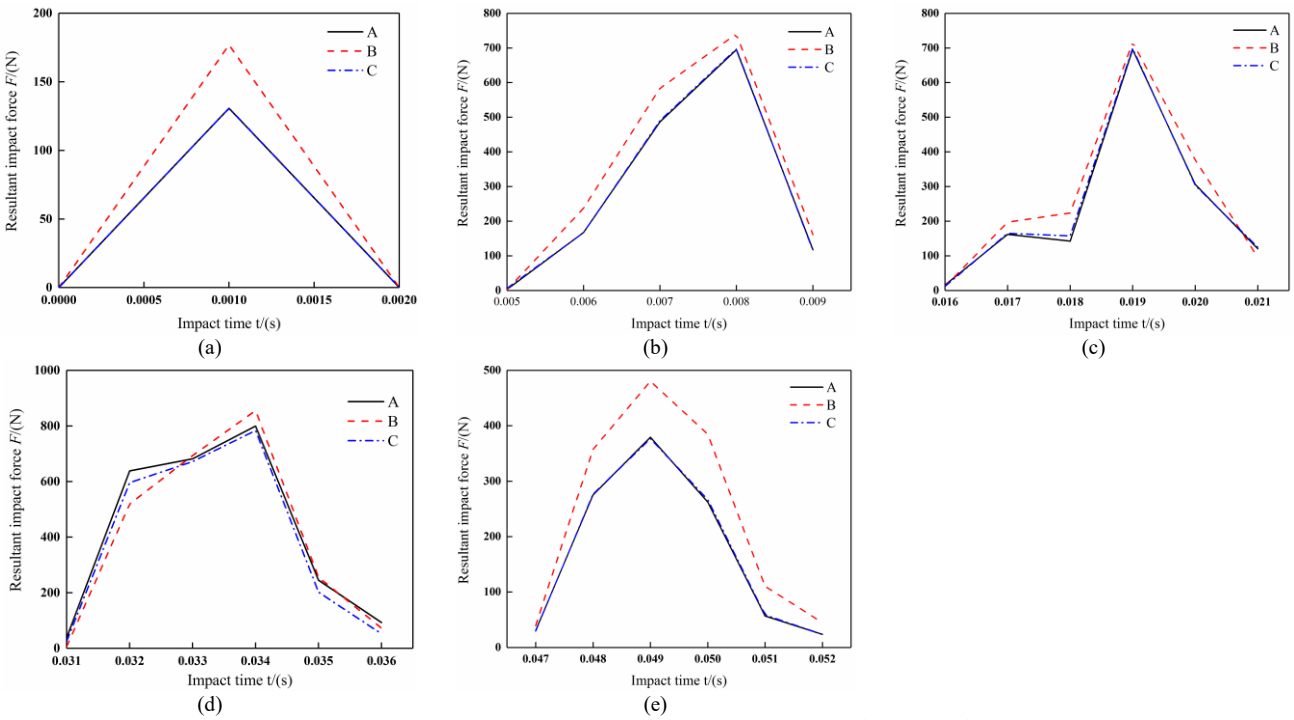

(a) ~ (e) represents No. 1, No. 6, No. 13, No. 19 and No. 24 tooth respectively

Figure 16. Resultant impact force along tooth width direction

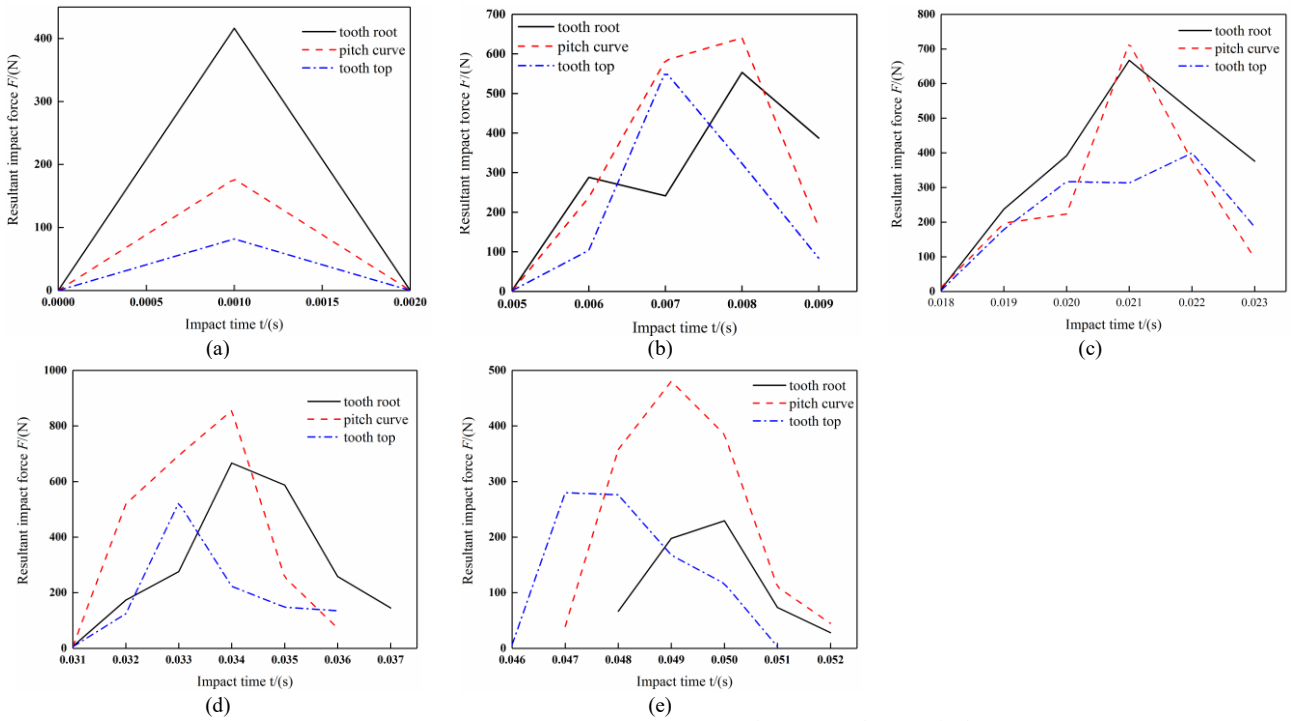

(a) ~ (e) represents No. 1, No. 6, No. 13, No. 19 and No. 24 tooth respectively

Figure 17. Resultant impact force along tooth height direction

Figure 17 shows the distribution trend of the resultant impact force along the tooth height direction. Except for the No. 1 tooth, the resultant impact force is the largest in the area near the pitch curve, and gradually decreasing from the pitch curve area to the tooth root and tooth tip area, Which is consistent with the analysis conclusion on cylindrical gears in the literature [9]. When defining contact, the No. 1 tooth is the first tooth that the driving gear and the driven gear contact, and its root part first contacts the tooth tip area of the driven gear. Due to the starting torque, the resultant impact force in the tooth root area is greater than the pitch curve and the tooth tip area. Generally speaking, the resultant impact force that each gear tooth bears during the meshing process is different, which is related to the inconsistency of the elliptic gear tooth profile. Through further summary, it can be concluded that the resultant impact force presents a distribution law that the two ends of the long axis increase to the ends of the short axis.

4.4. Analysis of impact time, maximum impact stress and resultant impact force

Figure 18 shows the impact time distribution trend under the impact stress and resultant impact force. In order to reduce the difficulty of analysis and simplify the analysis, only the teeth on the upper part of the elliptic pitch curve are given. The change trend of impact time under impact stress and resultant impact force is basically the same, and the impact time presents an increasing trend from No.1 tooth to No.24 tooth. The reason is that with the increase of the tooth number, the position of the tooth on the elliptic pitch curve is more and more far away from the center of rotation, which makes the meshing time of each tooth increase. It can also be explained by the time-varying transmission ratio of the elliptic gear. In general, the impact time under the impact stress and the resultant impact force increases from the near focus to the far focus of the elliptic curve.

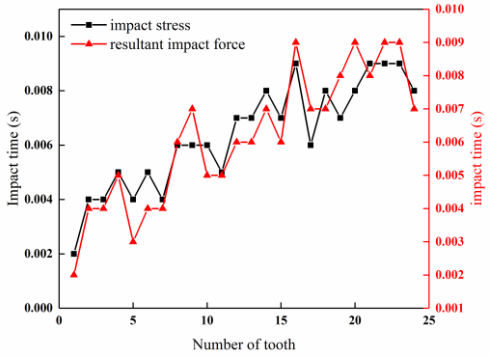

Figure 18. Impact time of single tooth

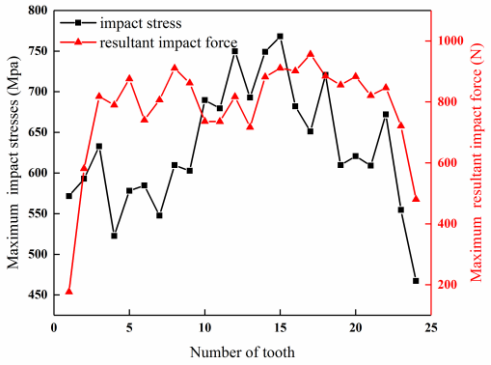

Figure 19. Distribution of maximum impact stress and maximum resultant impact force

The variation trend of the maximum resultant impact force and the maximum impact stress along the position of the gear tooth on the elliptic pitch curve is shown in Figure 19. The change trend of resultant impact force is more obvious, showing a gradual increase along the two ends of the long axis of the elliptic pitch curve to the two ends of the short axis. In contrast, the variation of maximum impact stress is more complex. The reason is that the tooth profile of elliptic gear is different from each other in the meshing process, which makes the impact stress of each tooth profile different. But it still presents a trend of gradual increase from the two ends of the long axis of the elliptic pitch curve to the two ends of the short axis. Although there is a slight decrease in the maximum impact stress of some teeth, the overall trend remains unchanged.

5. Conclusions

This article uses finite element analysis method to solve problems such as difficult to obtain contact impact and contact stress on the tooth surface of elliptic gears, and incomplete dynamic performance analysis theory. The dynamic distribution laws of contact stress, impact stress, impact resultant force, and impact time of elliptic gears were elaborated in detail.

1. The contact area of the tooth surface of the elliptic gear is ellipse. The maximum contact stress on the tooth surface of an elliptic gear occurs at the node of the single tooth contact area.
2. Along the direction of the tooth profile, the impact stress shows a gradually increasing distribution trend from the root to the top of the tooth. The resultant impact force shows a distribution pattern where the area near the pitch curve is the largest, and gradually decreases from the pitch curve area to the root and top areas of the teeth.
3. As the position of the gear teeth on the elliptic pitch curve varies, both the impact stress and the combined resultant impact force show a gradually increasing trend from both ends of the long axis of the elliptic pitch curve to both ends of the short axis.
4. The impact time shows an increasing trend from the near focal point of the elliptic nodal curve to the far focal point.

Funding

The research was support by the Gansu Province Youth Science Foundation Project of China (23JRRA751) and Gansu Provincial Department of Education of China: Innovation Fund Project for University Teachers (2023A-021).

References

[1] W. C. Smith, “The math of noncircular gearing”. Gear Technology, Vol.17, No.4, 2000, pp.18-21.
[2] B. Li, D. Chen, “Design, manufacture, inspection and application of non-circular gears”. Chinese Journal of Mechanical Engineering, Vol.56, No.9, 2020, pp.55-72.
[3] C. B. Dong, Y. P. Liu, Y. Q. Wei, “Dynamic contact characteristics analysis of elliptic cylinder gear under different load conditions”. J. Huazhong Univ. of Sci. & Tech. (Natural Science Edition), Vol.48, No.8, 2019, pp.103-107.
[4] J. Y, Tang, X. Liu, J. Dai, “Study on corner contact shock of gear transmission by ANSYS/LS-DYNA software”. Journal of Vibration and Shock, Vol.26, No.9, 2007, pp.40-44.
[5] R. G. Munro, L. Morrish, D. Palmer, “Gear transmission error outside the normal path of contact due to corner and top contact”. Proceedings of the Institution of Mechanical Engineers, Part C: Journal of Mechanical Engineering Science, Vol.213, No.4, 1999, pp.389-400.
[6] P. Ziegler, P. Eberhard, B. Schweizer, “Simulation of impacts in gear trains using different approaches”. Archive of Applied Mechanics, Vol.76, 2006, pp.537-548.
[7] T. Lin, H. Ou, R. Li, “A finite element method for 3D static and dynamic contact/impact analysis of gear drives”. Computer Methods in Applied Mechanics & Engineering, Vol.196, No.9, 2007, pp.1716-1728.
[8] C. Zhou, J. Tang, Z. Zhong, “Cornet contact and impact friction of gear drive”. Chinese Journal of Mechanical Engineering, Vol.44, No.3, 2008, pp.75-81.
[9] Tang J, Zhou W, Cheng S, “Contact-impact analysis of gear transmission system”. Chinese Journal of Mechanical Engineering, Vol.4, 2011, 22-30.
[10] Al-shyyab A, Alwidyan K., Ali M, et al., “Non-linear Dynamic Behaviour of Compound Planetary Gear Trains: Model Formulation and Semi-Analytical Solution”, Proc. IMechE, Part K: Journal of Multi-body Dynamics, Vol. 223, No.3, 2009, 199-210.
[11] S. Ahmad, K. Ahmet, “A Nonlinear Torsional Dynamic Model of Multi-Mesh Gear Trains Having Flexible Shafts”, Jordan Journal

of Mechanical and Industrial Engineering, Vol.1, No.3, 2007, pp.31-41.

[12] Q. Y. Zhang, Y. Wang, W. Liu, "Contact Mechanics Analysis and Optimization of Shape Modification of Electric Vehicle Gearbox", Jordan Journal of Mechanical and Industrial Engineering, Vol.14, No.1, 2020, pp.15-24.

[13] N. Gao, C. Meesap, S. Wang, "Parametric vibrations and instabilities of an elliptic gear pair". Journal of Vibration and Control, Vol.26, No.3, 2020, pp. 19-20."

[14] B. Dong, Y. P. Liu, Y. Q. Wei, "Research on the effect of rotation speed on the meshing characteristics of elliptic cylindrical gears". Jordan Journal of Mechanical and Industrial Engineering, Vol.14, No.3, 2020, pp.271-277.

[15] M. Emad, R. Ibrahim, "An application of finite element method and design of experiments in the optimization of sheet metal blanking process". Jordan Journal of Mechanical and Industrial Engineering, Vol.2, No.1, 2008, pp.53-63.

[16] "A. Arumugam, A. Pramanik, "Review of experimental and finite element analyses of spot weld failures in automotive metal joints". Jordan Journal of Mechanical and Industrial Engineering, Vol.14, No.3, 2020, pp.315-337.

[17] F. Alfaqs, "Dynamic behavior of thin graphite/epoxy frp simply supported beam under thermal load using 3-d finite element modeling". Jordan Journal of Mechanical and Industrial Engineering, Vol.15, No.3, 2021, pp.301-308.

[18] H. M. Tlilan, A. M. Jawarneh, A. S. Al-Shyyab, "Strain-Concentration factor of cylindrical bars with double circumferential u-notches under static tension".Jordan Journal of Mechanical and Industrial Engineering, Vol.3, No.2, 2009, pp. 97-104.

[19] M. Al-Mukhtar, S. Henkel, H. Biermann, "A finite element calculation of stress intensity factors of cruciform and butt welded joints for some geometrical parameters". Jordan Journal of Mechanical and Industrial Engineering, Vol.4, No.5, 2010, pp. 236-245.

[20] X. Wang, S. Wu, J. Chen, "Dynamic surface wear characteristics in spur gear transmission system with dynamic loads and wear coefficients". Journal of Central South University (Science and Technology), Vol.45, No.2, 2014, pp.408-413.

[21] John Argyris, B. Alfonso Fuentes, L. J. Faydor, "Computerized integrated approach for design and stress analysis of spiral bevel gears". Computer Methods in Applied Mechanics & Engineering, Vol.191, No.12, 2002, pp.1057-1095.

[22] W. B. Biing, "Tooth profile generation and analysis of crowned elliptic gears". Journal of mechanical design, Vol.7, no.131, 2009, 074503.